The On−Off Contrast in an All Optical Switch Based on Stimulated Raman Scattering in Optical Fibers[1]

A. Flores-Rosas[a],*, **E. A. Kuzin**[b], **B. Ibarra-Escamilla**[b], **and J. M. Merlo-Ramírez**[c]

[a] *Instituto Tecnológico Superior de Poza Rica, Luis Donaldo Colosio Murrieta S/N, Poza Rica, Ver. 93230, México*
[b] *Instituto Nacional de Astrofisica, Optica y Electronica, Optics Deparment, Luis Enrique Erro 1, Puebla, Pue. 72000, México*
[c] *Tecnológico de Monterrey, Campus Puebla, Vía Atlixcayotl 2301, San Andrés Cholula, Pue, 72800, México*
*e-mail: arielf@nucleares.unam.mx
Received February 14, 2012; published online July 9, 2012

Abstract—We present the investigation of the ON−OFF contrast in an optical switch using stimulated Raman Scattering in optical fibers. The setup consists of a Raman circuit of two fiber stages connected in series with a spectral filter rejecting the signal inserted between them. The stage 1 works as saturated amplifier, in this stage the pump pulses are saturated when pump and signal are launched to the input or travel through the fiber without saturation when pump only is launched at the input. The stage 2 works as a Raman amplifier with amplification depending on the pump power entering from the first stage. When pump only is launched at the input enter to the second stage without saturation and amplifies the signal entering this stage, strong signal pulses appear at the output; when pump and signal are launched to the input the pump is saturated in the first stage and the filter rejected the amplified signal, so that only low power pump enters the second stage and no signal pulses appear at the output. We use 2 ns pump pulses at 1528 nm and continuous-wave signal at 1620 nm. In the first stage of Raman circuit, we use both fibers with normal and anomalous dispersion. In fibers with anomalous dispersion, pump saturation is affected by modulation instability. We find that the contrast may be improved using fibers with normal and anomalous dispersion connected in series in the first stage, provided there is appropriate selection of their lengths. The best achieved contrast was 15 dB at 6 W pump peak power.

DOI: 10.1134/S1054660X12080099

1. INTRODUCTION

The data processing devices in the all-optical domain whose operation relies on nonlinear optical phenomena has been of considerable interest in recent years as an alternative to electronic switching in optical communication systems [1, 2]. These devices have a strong potential for a variety of applications in such diverse areas as ultrahigh-speed optical telecommunications, ultrafast metrology, optical sensing, microwave engineering and optical computing. In literature, multiple principles and devices have been presented; among them a great part is embodied by devices based on the Kerr effect in fiber, such as the well-known nonlinear optical loop mirror (NOLM) originally proposed in [3], devices based on cross phase modulation (XPM) and four-wave mixing (FWM) [4, 5], logic gates [6] and wavelength conversion [7]. Owing to its self-switching ability and flexibility, the NOLM has been recognized as a valuable tool in a large field of optical signal processing applications. These include optical soliton switching [8], wavelength demultiplexing [9], mode locking [10], etc. The NOLM as well as other interferometric devices provide an oscillating power transfer function while the ideal characteristic is the steplike function. The power transfer function of the FWM-based devices approaches the steplike func-

tion; however, for a single-stage scheme, a flat response is achieved only at spaces while at marks an oscillating dependence was measured [11]. A double stage scheme demonstrates flat response at both spaces and marks [12].

Up to day one of the most important nonlinear effects that is presented in optical fibers is Stimulated Raman scattering (SRS). However there are only few works discussing the application of the SRS for signal regeneration and optical switch. Furthermore, SRS can be expected to present several advantages because of high amplification of the signal and intrinsic compatibility with communications systems employing Raman amplification of signals [13]. The design of Raman circuits can be based on the strong dependence of the Raman amplification on pump power that was considered for wavelength conversion with high extinction ratio [14]. With this approach, output signal pulses at Stokes wavelength are generated as a result of the Raman amplification caused by input signal pulses used as the pump. Because of the strong dependence of Raman amplification on pump power, the extinction ratio of the output signal can be much higher than that of the input signal. A second approach exploits pump saturation in presence of the signal [15]. In this case, the pulses at Stokes wavelength are used as an input signal, whereas the pump pulses are considered as an output signal. In the absence of the Stokes
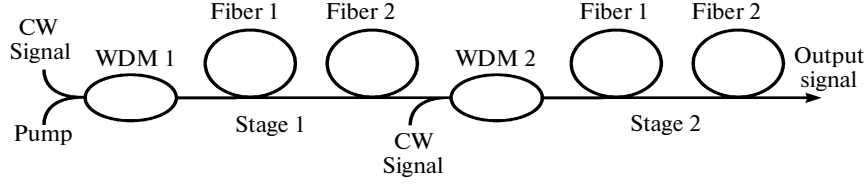
Fig. 1. Setup of Raman circuit.

pulse (spaces), the pump pulse passes through the fiber without saturation and has high power at the fiber output (marks), whereas in presence of the Stokes pulse (marks) the pump pulse is depleted and has a low power at the fiber output (spaces). However, both approaches do not provide a desirable steplike power transfer function. The combination of the Raman amplifier (where the pump is saturated by signals) and Raman amplifier (where the signal pulse is used as the pump) was also considered in connection with the recirculation loop, where the signal can travel in the closed fiber loop without degradation during an infinitively long time [16]. In this paper, we consider, theoretically and experimentally, the Raman circuit using the approach suggested in [16] and show that it allows the steplike power transfer function with high differential gain and low input signals. We find that the effect of modulation instability may degrade the operation of the device and show how this degradation can be avoided.

2. THEORETICAL ANALYSIS

In this section we present simple numerical calculations to show the basic principles and potential of the approach. Figure 1 presents the diagram of the Raman circuit, it consists of two stages. The stage 1 works as saturated amplifier where the pump pulses are saturated if the signal is at "Marks" or travel through the fiber without saturation if the signal is at "Spaces." The stage 2 works as a Raman amplifier with amplification, depending on the pump power entering from the first stage. If the input signal is at spaces, then the pump enters the second stage without saturation and generates high power at Stokes wavelength (i.e., the output signal is at Marks). If the input signal is at "Marks," then the pump is depleted in the first stage and in the input the output signal is at "Spaces." So the circuit operates as an inverter. For this operation to be allowed the pump power has to be high enough to provide strong amplification of the signal, and simultaneously lower than the SRS threshold at which strong Stokes pulses and pump depletion appears as a result of the amplification of the initial spontaneous Stokes waves. The wavelength shift between Signal and Pump has to be close to the maximum Raman gain (about 110 for 1550 nm band). The wavelength of the cw seeding laser wave defines the wavelength of the output signal. It may not be the same as the wavelength

of the input signal that provides the possibility of the wavelength conversion. Because of the big difference between pump and signal wavelengths the walk-off between pump and Stokes is inevitable. To avoid the degradation of the operation because of walk-off effect the dispersion management can be used connecting the fibers in which the signal travels faster than pump with the fibers in which the signal travels slower than pump. If the fibers with anomalous dispersion are used, the modulation instability (MI) can be expected, which will complicate drastically circuit operation.

To illustrate the operation principle, we evaluated the Raman circuit on the basis of the coupled equation for pump, A_P, and Stokes, A_S, pulses,

$$\frac{\partial A_S(t)}{\partial z} + (1/V_P - 1/V_S)\frac{\partial A_S(t)}{\partial t}$$

$$+ i\frac{\beta_2}{2}\frac{\partial^2 A(T, z)}{\partial t^2} = \frac{g}{2}A_S(t)|A_P(t)|^2, \qquad (1)$$

$$\frac{\partial A_P}{\partial z} + i\frac{\beta_2}{2}\frac{\partial^2 A_P(T, z)}{\partial t^2} = -\frac{g}{2}A_P|A_S|^2,$$

where β_2 is the GVD parameter considered equal for pump and Stokes wavelengths; g is the Raman gain coefficient equal to 10^{-13} m/W for silica glass at 1550 nm wavelength; V_P and V_S are the group velocity of pump and Stokes pulses respectively. Here, we do not consider the effects connected with nonlinear Kerr effect to provide the simplest explanation of the basic principles. However, this effect may be important, especially in fibers with anomalous GVD, because it may cause the modulation instability and pulse breakup. The calculations were done with the split-step Fourier method. The parameters of the fibers used in calculations in most cases correspond to those of the fibers used in our experiments: Fiber 1 is a Corning SMF-LS dispersion shifted fiber with normal dispersion $D = -6$ ps/nm/km at 1550 nm; Fiber 2 is a standard SMF-28 fiber with anomalous dispersion $D = 20$ ps/nm/km; Fiber 3 is an OFS True Wave fiber with anomalous dispersion $D = 8.9$ ps/nm/km. Figure 2 shows characteristic examples of the pump pulses at the output of Fiber 1 (Fig. 2a) and at the output of Fiber 2 (Fig. 2b). Input pulse is also shown by solid line.
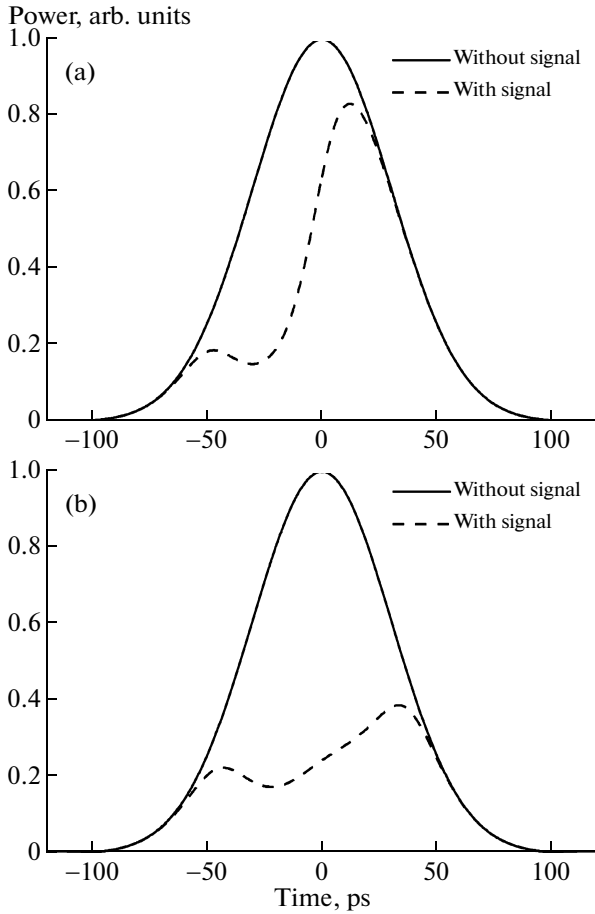
Power, arb. units

Fig. 2. Input (solid line) and output (dashed line) waveforms of the pump at the end of (a) Fiber 1 and (b) Fiber 2.

Fig. 3. Energy of Stokes pulses at the output of the circuit.

The parameters of the setup used for calculations were the following, as the Fiber 1 is 100-m of SMF-LS fiber; as the Fiber 2 is 25-m SMF-28 fiber. The 25 W pump pulse presents the Gaussian shape with a duration equal to 100 ps measured as FWHM. The input Stokes pulse has a super Gaussian shape with a pulse duration equal to 300 ps and a peak power equal to 1 mW and effective area of fibers of 50 μm². The Fiber 1 has normal dispersion so the Stokes pulse has a higher speed and the leading edge of the pump pulse reveals stronger depletion tan the trailing edge. The depletion can be done stronger when the fiber with normal dispersion is spliced with a fiber with anomalous dispersion, Fig. 2b.

The dependencies of the energy of the output signal pulse on the input signal power are presented in Fig. 3 for three different configurations of the Stage 1. The energy is scaled with respect to the energy of the output signal when no signal enters from the input. The solid line represents the switch when Stage 1 comprised only Fiber 1 with 295 m of length. The dashed line represents the case when Stage 1 comprised three fibers connected in series: 150 m of Fiber 1, 45 m of
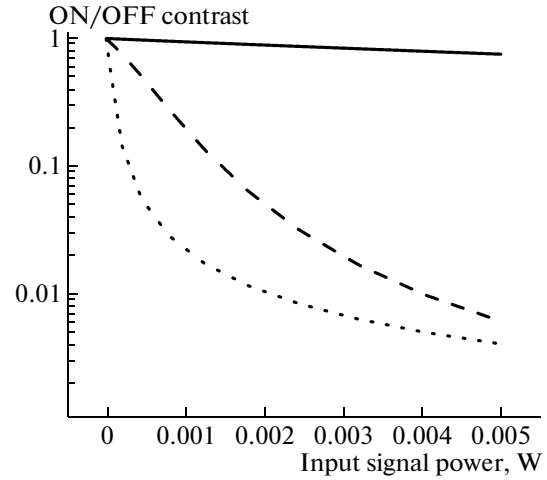
Fiber 2, and 100 m of Fiber 3. The dotted line shows the results when the first stage comprised 295 m of Fiber 3. For all cases 350 m of Fiber 3 was used for Stage 2. As we can expect the result depends drastically on the walk-off. The best result is provided by the fiber with low dispersion. In practice it may not be very easy to fulfill the condition that the walk-off length be longer than the fiber length especially if low power and thus a long fiber is required, however a simple dispersion management technique using only three lengths of fibers with normal and anomalous dispersion may provide switching with a contrast (the ratio between the energies of the signals at the second stage output when the input signal is "Spaces" and "Marks") of about 20 dB at input power less than 10^{-3} of pump power.

Strong dependence of the output signal energy on the input signal power allows the improvement the signal/noise ratio of signals. In order to prove this we added Gaussian noise to the input Stokes pulse. We considered two possibilities: only noise is launched into Fiber 1 (input signal "off"); a Stokes pulse with noise is launched into Fiber 1, input signal "on." The scaled power shows the ratio between the signal power and the peak power of the pump pulse. The Stokes pulse at the output of Fiber 3 was calculated for both cases. Figure 4 shows 10 Stokes pulses for input signal "on" and 10 Stokes pulses for input signal "off" when random noise is applied. The parameters of the setup used for calculations were the following: Fiber 1 is the 100 m SMF-LS; Fiber 2 is the 40 m SMF-28; Fiber 3 is the 300 m True Wave fiber; input pump power is 24 W; input signal power is 1 mW. As we can see the output Stokes pulses corresponding to input signals "ON" and "OFF" are very well distinguished.

These simple presented considerations show that the Raman circuit allows effective optical switching, logic operation, and noise reduction with signal power as low as 10^{-3} of the pump power. However, there are
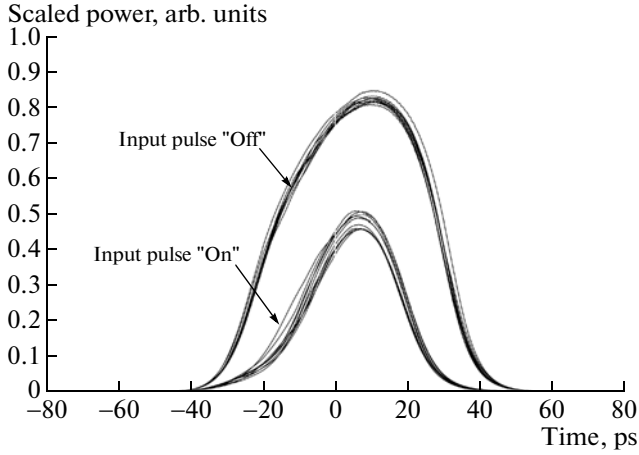
3. EXPERIMENTAL RESULTS

Scaled power, arb. units

Fig. 4. Output Stokes pulses for input pulses "ON" and "OFF."

several effects that will affect the Raman circuit operation and must be considered. As we have seen, the connection in series of fibers with normal and anomalous dispersions allows a strong improvement of the operation of the circuit. However, in fibers with anomalous GVD, the effects of MI and pulse breakup appear at powers lower than that required for strong Raman amplification [17]. It can be expected that pulse breakup will affect the depletion of the pump pulse and amplification of the Stokes pulses. The principal characteristics of the circuit are the pump pulse duration and power, and the signal pulse duration and power. The delay time, depending on the fiber length indeed does not affect the bandwidth of the circuit. The principal limit of the pulse duration is defined by the response time of the Raman effect and lies in the femtosecond scale. However, for reasonable pump powers and fiber parameters, the limit of the pulse duration is defined by the walk-off between pump and signal rather than by the response time. We numerically show the operation for 100 ps pulses and fiber parameters corresponding to widely available fibers. However, the development of the photonics crystal fibers allows fabrication of the fibers with very high flexibility of the dispersion characteristic and nonlinear properties. The use of pulses with several picoseconds of duration and <1 W of power can be easily expected.

The experimental setup of Raman circuit is pictured in Fig. 5. Our system used as a source of pump pulse a diode laser with $\lambda = 1528$ nm. This diode laser is directly modulated by the pulse generator SRS DG535 to generate pulses with duration of 2 ns. The pulses from the diode laser with power of several mW are amplified by an EDFA to the power of several tens of watts. The pump pulses are introduced to the 85/15 Coupler 1, whose 85% port is spliced with the first stage comprising Fiber 1 + Fiber 2. As the Fiber 1 we used the Corning SMF-28 fiber with anomalous GVD equal to 20 ps/nm-km, as the Fiber 2 we used the Corning SMF-LS dispersion shifted fiber with GVD equal to −6 ps/nm-km (normal dispersion at pump wavelength). The cw radiation with wavelength equal to 1620 nm is also introduced into the Coupler 1 and 15% of this power enters the first stage. In experiments the signal power introduced into Fiber 1 was 0.5 mW. The polarization controller inserted after the EDFA allows adjusting the polarization of the pump to provide a maximum Raman amplification in the fibers because the Raman amplification depends on polarization states of Pump and Stokes [18, 19]. The Fabry−Perot (FP) filter was used to reject the 1620 nm radiation at the end of the first stage. The transmission of the FP filter for 1528 nm radiation was −4 dB. The 90/10 Coupler 2 was used to launch the 1528 nm pump pulses and 1620 nm CW signal to the second stage of the Raman circuit. The signal power launched into the Fiber 3 was about 0.5 mW. As the Fiber 3 we used 4.5 km of OFS True Wave (RS) fiber. With this configuration we were able to measure simultaneously the pump pulse at the input of the first stage, the pump at the output of the first stage and the Stokes or pump pulses at the output of the second stage.

As it can be seen from the simulation the process of the pump saturation in the first stage is very important for the circuit operation. We investigated the pump saturation in the first stage for different span of the Fiber 1 and Fiber 2. Figure 6 present the waveforms of pump pulses at the output of the FP filter for different pump powers when only the Fiber 1 was used in the first stage. Figure 6a was obtained with a fiber length of 300 m and the inset is for the fiber with length of 600 m, and Fig. 6b with fiber length of 1 km. Strong depletion of the pump pulse was observed for the
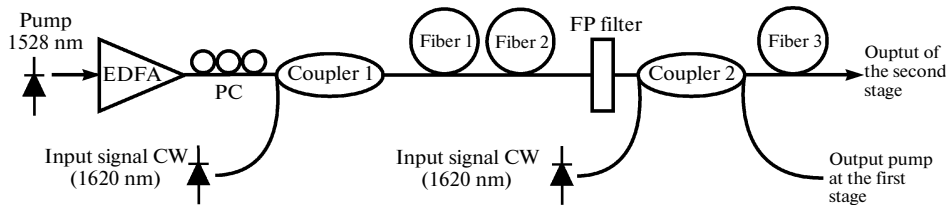

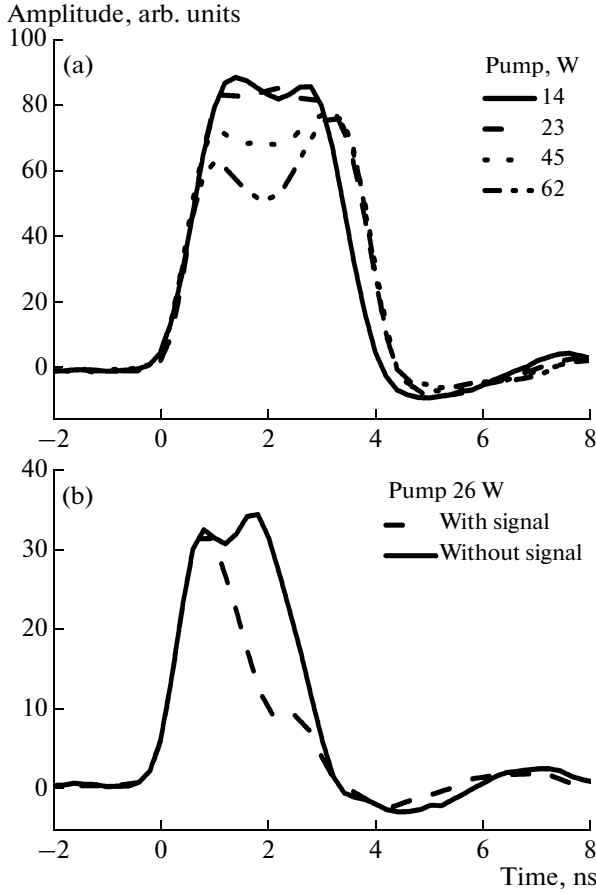**Fig. 5.** Experimental setup of raman circuit.

Fig. 6. Pump pulses at the output of the FP filter when the SMF-28 fiber was used as the Fiber 1; (a) fiber length is equal to 300 m y 600 m; (b) fiber length is equal to 1 km.

Fig. 7. (a) Saturation of the pump by the input signal with 350 m of SMF-LS fiber for 31 W and the inset for 35 W pump power and (b) for 550 m SMF-LS for 20 W and the inset for 25 W pump power.

300 m and 600 m of fiber even if the 1620 nm radiation was not applied. In this case, the effect of the 1620-nm radiation on the pulse depletion was not detected. The maximum power at the FP output was measured to be equal to 7 W for 300 m and 3 W for 600 m. The pump depletion is caused by the pulse breakup process followed by the soliton self-frequency shift that results in broadening of the spectrum and the decrease of the power at the output of the FP filter. For 1 km fiber the depletion caused by the pulse breakup also was observed however some effect of the 1620 nm radiation was detected. The pump power for Fig. 6b is 26 W. We measured the Raman amplification and calculated the dependence of the Raman gain with the fiber length for SMF-28 fiber. The 0.5 mW 1620 nm is launched to the fiber. The pump is on 1528 nm and Stokes is on 1620 nm. The Raman gain average experimental value = 0.72 W^{-1} km^{-1} and theoretical value for linearly polarized pump and Stokes = 0.72 W^{-1} km^{-1}. Theoretical calculations agree well with experimental.

The experiment using the SMF-LS fiber with normal dispersion shows conventional saturation of the pump that corroborates well the simulations based on
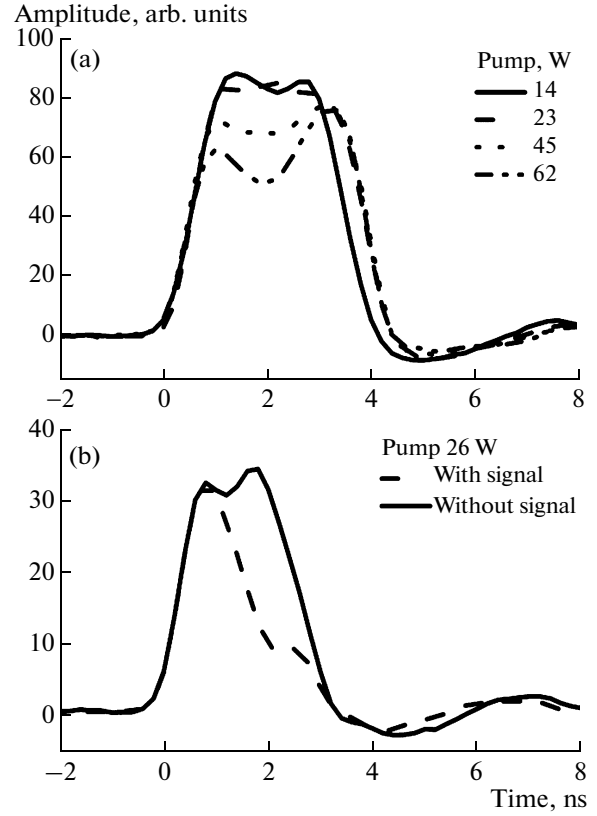
Eq. (1). Figure 7 presents the results for a fiber of 350 and 550 m length. At pump power equal to 31 W and the inset of 35 W for 350 m of SMF-LS, Fig. 7a; at pump power equal to 20 Wand the inset of 25 W for 550 m of SMF-LS, Fig. 7b. Without input signal no change in the waveform of the pump pulse is observed for Figs. 7a and 7b.. However at 0.5 mW signal input power strong depletion can be seen on the Figs. 7a and 7b. At 35 W for 350 m of SMF-LS and 25 W for 550 m of SMF-LS pumps power the depletion is observed even without input signal, see insets of Fig. 7. In these case a strong Stokes pulse at 1635 nm was detected which causes the pump depletion. In conventional terms this means that the pump power is higher than the threshold power. However in this case a strong effect of the input signal can still be seen.

The composed fiber consisting of the span of SMF-LS spliced with the span of SMF-28 was also tested. The saturation of the pump by input signal was observed if the length of SMF-LS is at least two times longer than the length of the SMF-28. In this case the power required for MI is higher than that required for effective pump depletion. Figure 8 presents an example of the output pump pulses at the end of the first
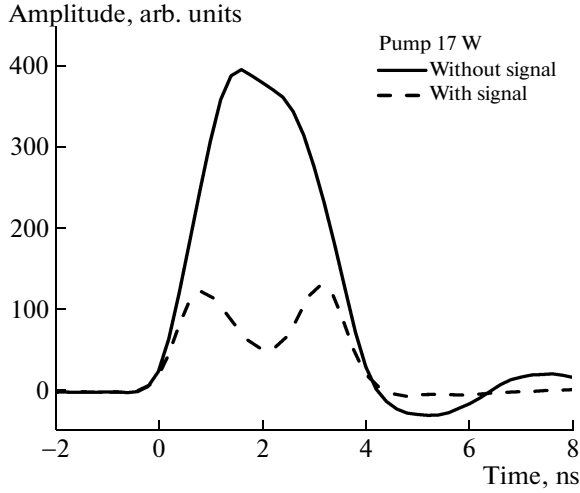
Amplitude, arb. units

Fig. 8. Saturation of the pump by the input signal if the first stage comprises a 550 m SMF-LS fiber connected to a 300 m SMF-28; pump power is 17 W.
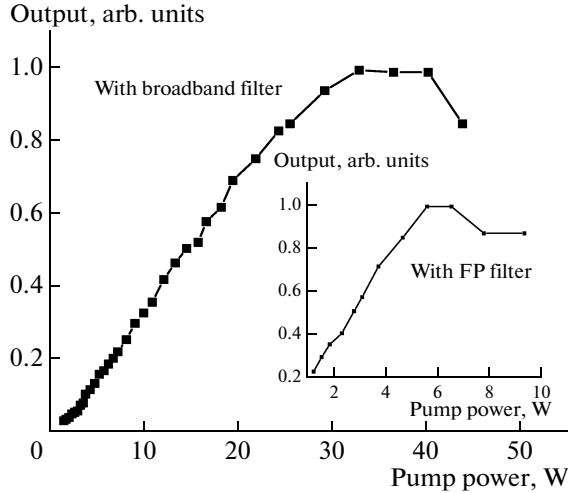
Output, arb. units

Fig. 9. Saturation of pump measured with narrowband and broadband filter.

Amplitude, arb. units

Fig. 10. The waveforms of the signal at 1620 nm at the output of Fiber 3; dashed line—input signal "OFF," solid line—input signal "ON." The first stage consists of the 350-m of the SMF-LS fiber—(a); the first stage consists or of the 350-m SMF-LS connected to the 600-m SMF-28—(b). The inset shows the Energy of Stokes pulses, (a) for 350 m SMF-LS in the first stage; (b) for 350 m SMF-LS + 600 m SMF-28 in the first stage.

stage which consisted from a 550 m span of SMF-LS and a 300 m span of SMF-28.

If the pump depletion in the first stage composed from the SMF-28 is determined by MI the results of the depletion has to be dependent on the bandwidth of the filter inserted between the first and the second stages. To prove this we used as a broad band filter a span of the SMF-28 wounded on a cylinder with a diameter of 16 mm. For small radius of curvature, a strongly wavelength-dependent loss appears. For our case the loss of the fiber with curvature was measured to be 18 dB for 1620 nm and 5.5 dB for 1528 nm. The difference between losses is sufficient to measure the depletion of the pump with this broad band filter. Figure 9 represents the results of the depletion measurement with the FP filter with bandwidth of 1 nm, and
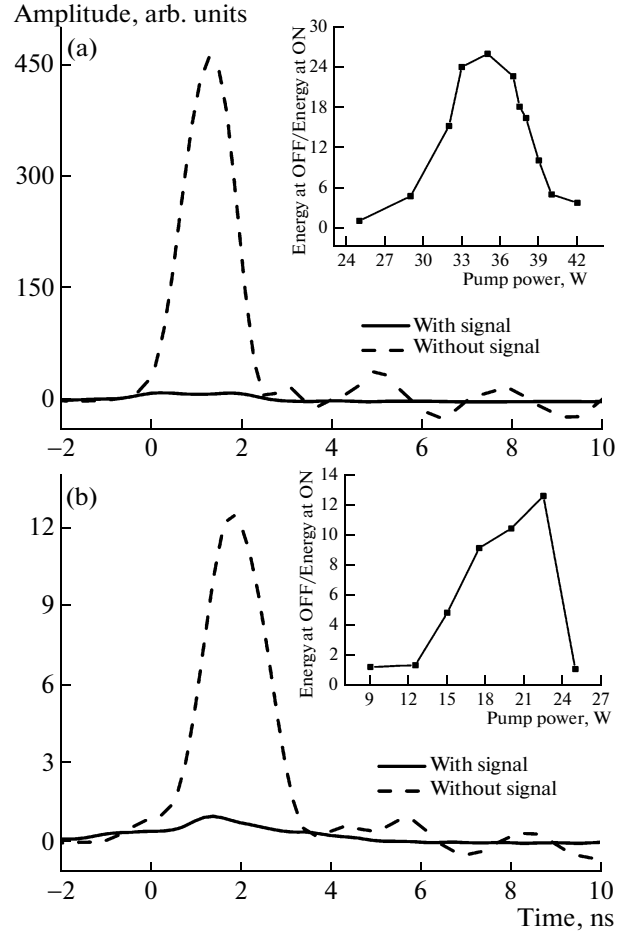
the inset with the broadband filter. It can be clearly seen that with the narrow band filter the pump depletion appears at approximately 5 W of pump power while with the broad band filter the pump depletion appear at 30 W of input power. These results show that the problem connected with the MI could be overcome using the broad band filter between the first and second stages. It could be for example a filter based on a liquid-filled Photonic Crystal Fiber [20] with step-like dependence of transmission on the wavelength.

Finally we tested the two-stage setup. In the second stage we used a 4.5-km OFS True Wave (RS) fiber. In the first stage we used different combinations of the dispersion shifted Corning SMF-LS fiber and Corning SMF-28 fiber. Figure 10 shows examples of the waveforms of the signal pulses at the output of Fiber 3. The results of Fig. 10a were obtained with 350 m of SMF-LS as the first stage at 33 W pump power; the

results of Fig. 10b were obtained with 550 m of SMF-LS spliced with 600 m of SMF-28 used as the first stage at 21 W pump power. The inset of Fig. 10 shows the dependencies of the contrast on the pump power. The contrast was measured as the ratio between the energies of the signals at the second stage output when the input signal is "OFF" and "ON." The dependencies are shown for the first stage consisting of the 350-m SMF-LS fiber, inset Fig. 10a, and for the first stage consisting of the 350-m SMF-LS and the 600 m SMF-28 fiber, inset Fig. 10b.

4. CONCLUSIONS

The use of SRS to design an all optical switch circuit makes it possible to use very low powers of signal to control respectively strong pulses. The principle of operation can be based on pump depletion because of the transference of energy from the pump to the first stokes. The pump depletion and respectively the on–off contrast are restricted by pulse shape and GVD. We investigated a two-stage setup and the dispersion management technique to improve the on–off contrast and have obtained experimentally the contrast equal to 15 dB for a signal power as low as 0.5 mW. We have found that the pump depletion in fibers with anomalous dispersion is deteriorated by the pulse breakup process so the use of the dispersion management technique requires the appropriately selection of the fibers with anomalous and normal dispersion.

ACKNOWLEDGMENTS

REFERENCES

1. N. Nishizawa and Y. Ukai, Opt. Express **13**, 8128 (2005).
2. M. Bajcsy, S. Hofferberth, V. Balic, T. Peyronel, M. Hafezi, A. S. Zibrov, V. Vuletic, and M. D. Lukin, Phys. Rev. Letters **102**, 203902-1 (2009).
3. N. J. Doran and D. Wood, Opt. Lett. **13**, 56 (1988).
4. B. E. Olsson and D. J. Blumenthal, IEEE Photon. Technol. Lett. **13**, 875 (2001).
5. E. Ciaramella and T. Stefano, IEEE Photon. Technol. Lett. **12**, 849 (2000).
6. T. Fujisawa and M. Koshiba, J. Opt. Soc. Am. B **23**, 684 (2006).
7. R. Dekker, A. Driessen, T. Wahlbrink, C. Moormann, J. Niehusmann, and M. Först, Opt. Express **14**, 8336 (2006).
8. M. N. Islam, C. E. Soccolich, and D. A. B. Miller, Opt. Lett. **15**, 909 (1990).
9. A. I. Siahlo, L. K. Oxenløwe, K. S. Berg, A. T. Clausen, P. A. Andersen, C. Peucheret, A. Tersigni, P. Jeppesen, K. P. Hansen, and J. R. Folkenberg, IEEE Photon. Technol. Lett. **15**, 1147 (2003).
10. B. Ibarra-Escamilla, E. A. Kuzin, D. E. Gomez-Garcia, F. Gutierrez-Zainos, S. Mendoza-Vasquez, and J. W. Haus, J. Opt. A Pure Appl. Opt. **5**, 225 (2003).
11. E. Ciaramella, F. Curti, and S. Trillo, IEEE Photon. Technol. Lett. **13**, 142 (2001).
12. S. Yamashita and S. Mazumder, IEEE Phot. Tech. Lett. **18**, 1064 (2006).
13. C. Headley and G. P. Agrawal, *Raman Amplification in Fiber Optical Communication Systems* (Elsevier, Amsterdam,, 2005).
14. A. Uchida, M. Takeoka, T. Nakata, and F. Kannari, Lightwave Tech. **16**, 92 (1998).
15. F. Ahmed and N. Kishi, Optical Rev. **10**, 43 (2003).
16. V. I. Belotitskii, E. A. Kuzin, M. P. Petrov, and V. V. Spirin, Electr. Lett. **29**, 49 (1993).
17. G. P. Agrawal, *Nonlinear Fiber Optics* (Academic, New York, 2001).
18. Q. Lin and G. P. Agrawal, J. Opt. Soc. Am. B **20**, 1616 (2003).
19. S. Sergeyev, S. Popov, and A. T. Friberg, Opt. Communs. **262**, 114 (2006).
20. S. Torres-Peiró, A. Díez, J. L. Cruz, and M.V. Andrés, Opt. Lett. **33**, 2578 (2008).